Vercelli Natalia (Orcid ID: 0000-0002-3150-9905)

Ares María Guadalupe (Orcid ID: 0000-0002-6992-6974)

Linking soil water balance with flood spatial arrangement in an extremely flat landscape

Natalia Vercelli[1,2] (corresponding autor: nvercelli@ihlla.org.ar)

Marcelo Varni[1]

Bruno Lara[2,3]

Ilda Entraigas[1,5]

María Guadalupe Ares[1,2]

[1]Instituto de Hidrología de Llanuras 'Dr. E. J. Usunoff', 780 República de Italia Avenue, B7300, Azul City, Buenos Aires Province, Argentina.

[2]Consejo Nacional de Investigaciones Científicas y Técnicas, 1917 Rivadavia Avenue, C1033AAJ, Autonomous City of Buenos Aires, Argentina.

[3]Laboratorio de Investigación y Servicios en Teledetección de Azul (LISTA), Facultad de Agronomía, Universidad Nacional del Centro de la Provincia de Buenos Aires, 780 República de Italia Avenue, B7300, Azul City, Buenos Aires Province, Argentina.

[4]Comisión de Investigaciones Científicas, Road 526 between 10 and 11, B1900, La Plata City, Buenos Aires Province, Argentina.

This article has been accepted for publication and undergone full peer review but has not been through the copyediting, typesetting, pagination and proofreading process which may lead to differences between this version and the Version of Record. Please cite this article as doi: 10.1002/hyp.13567

Linking soil water balance with flood spatial arrangement

Key words:

Floods

Spatial patterns

Landscape metrics

Soil water balance

Large plains

Argentine Pampas

Abstract:

In areas with very mild relief, water drains in a disordered way due to the lack of a developed drainage network, as it occurs in extremely flat sedimentary regions like the Argentine Pampas. The study analyzed the flood spatial arrangements in 2014 by calculating landscape metrics and relating them to soil water balance. The study area is located at Del Azul creek lower basin (Pampa Ecoregion, Argentina). Daily soil water balances were obtained, and 7 landscape metrics were calculated in 15 windows in 5 LandSat images, all along 2014, to explore the relationship between hydrological scenarios and spatial pattern summarized with Principal Component Analysis. Water excess concentrated in winter (June and August); deficits were in late spring and summer (January and November), while the beginning of autumn (March) was an intermediate situation. Principal Component 1 (44.7%) reflected area and shape metrics, and correlated positively with watertable level; Principal Component 2 (32.3%) summarized aggregation ones and was negatively associated with accumulated water excesses or deficits in previous 30 days, and useful reserve. Both exhibited possible threshold-driven behavior. Internal heterogeneity between NW and SE zones within the study areacoincided with the existence of ancient alluvial fans. The results highlight the peculiarities of the flood spatial patterns in regions with very mild relief, where landforms usually determine water flows.

Introduction

Analyzing the spatial and temporal variability of hydrological processes (Dingman, 2015; Western, Bloschl & Grayson, 2001) is a prerequisite for a more complete comprehension of their behavior, while allowing for more accurate predictions (Western et al., 2001). In this sense, Grayson and Blöschl (2000), Schröder (2006), Sivapalan (2005), Tetzlaff et al. (2007), and Van Nieuwenhuyse, Antoine, Wyseure and Govers (2011), among others, propose to analyze spatial variability in hydrological systems using an interdisciplinary approach to identify and quantify relevant spatial patterns, highlighting the application of geostatistical analysis and conceptual models of regional and landscape ecology. Landscape units form a mosaic organized in a quantifiable pattern, where each unit or patch is a discrete and limited portion which differs from its surroundings by structure or composition (Pickett & Cadenasso, 1995).

Extremely flat regions with low topographic gradients are among the least studied hydrological systems. In these regions, the familiar concept of runoff convergence to a single main stream is not applicable during floods, because the hydraulic capacity of conduction of the channels is very small and the floodplain is not well defined (Fuschini Mejía, 1994). As a result, water drains in a disordered, indefinite and unpredictable way, generating mantiform runoff (Jones, Poole, O' Daniel, Mertes & Stanford, 2007). In these systems, floods are characterized by being shallow (less than 1 m), large (tens or hundreds of km^2) and very long residence time in relation to the area of contribution (10-20 days) (Fan, Li & Miguez-Macho, 2013), in addition to generating the filling and chaining of low areas that produces a flow through the connection of surface storage. Long residence times are due to the low topographic gradients (minimum runoff) and to the shallow water table, which considerably reduces infiltration. Hence, surface storage losses depend mainly on evaporation.

Differently from regions with significant topography, where the choice of a hydrological model or another is often dictated by the way and scale in which we represent the topography (Grayson & Blöschl, 2000), the lack of flow convergence to an organized drainage network means that classic hydrological models, and their corresponding methodologies, are often inapplicable in flat plains (Scioli, 2009). Therefore, the correct simulation of surface runoff in areas of low slope is strongly dependent on a detailed topography (Scioli & Villanueva, 2011). Despite the availability of digital elevation models (SRTM 30m – Interferometric, Aster GDEM 30m – optic and TanDEM-X 12 m to 90 m Interferometric, among others) with low relative errors, its implementation in flat areas requires the application of correction strategies.

Mapping the subtle differences given by microtopography, even with instruments for precise measurement, is an arduous task that requires field survey of trees and areas with high vegetation, stream floodplains, anthropogenic communication channels, small runoff paths, etc. (Fajardo González, 2017). Finding similar areas is not easy since the subtle differences given by microtopography generate variability in the shape and connectivity of the sites with surface water during times of water excess (Bracken & Croke, 2007; Turnbull, Wainwright & Brazier, 2008), even when hydrological and topographic data are complemented with information about geomorphology, soil types and land use.

Large flood events are frequent in the Argentine Pampa Ecoregion (subhumid eolian plains of center-east Argentina), as well as in several regions around the world: the Pantanal in Brazil (Hamilton, 2002), the Orinoco Llanos in Colombia and Venezuela (Hamilton, Sippel & Melack, 2004), the plains of Manitoba and Saskatchewan in Canada, the Great Plains of Hungary (Jobbágy, Nosetto, Santoni & Baldi, 2008), and Western Siberia (Biancamaria, Bates, Boone & Mognard, 2009). Particularly in the Argentine Pampas, the landscape is characterized by scarce topographic slopes (less than 1% and even reaching values between 10^{-3} and 10^{-4}), low density of drainage network and significant development of lagoons of varying size (Aragón, Jobbágy & Viglizzo, 2010). This, added to the sub-humid climate (annual rainfall ranges between 700 to 1200 mm from SW to NE, and mean annual temperature ranges 14 to 20 °C, decreasing towards the south of the region), causes that basin boundaries are generally poorly defined, with a thick drainage texture. Potential evapotranspiration is around 800 mm, and this is why there is often an annual water excess (Pereyra, 2003), concentrated in the autumn-winter period. In spite of this, great interannual climatic variability is observed, as it happens throughout the south of the American continent (Garreaud, Vuille, Compagnucci & Marengo, 2009), causing a high risk of flooding during wet periods.

This extensive aggradational plain of 400,000 km^2 harbors the most important grassland ecosystem in Argentina (Matteucci, 2012) and more than 50% of the total population (INDEC, 2010). The Pampas region yields 90% of the national production of grains (mainly soy, wheat, corn and sunflower) and breeds 13 million heads of cattle (INDEC, 2008; Magrin, Travasso & Rodríguez, 2005). Despite its productive capacity, the alternation of dry and humid periods that historically has occurred in the region causes significant economic losses in the agricultural sector (Scarpati & Capriolo, 2013).

The subtle differences of topography, added to the high productive capacity of the region, justify the need to analyze the spatial configuration of floods and their spatio-temporal variability in extremely flat areas.

Characterizing spatial patterns provides information that can be complementary to the parameters traditionally used in hydrological models for the definition of hydrological response units (topography, coverage, slope, soil types, land use). Therefore, the aims of this study are: 1. to estimate daily soil water balance during a year with water excess, 2. to evaluate flooding patterns in a representative plain landscape in contrasting hydrological situations and, 3. to analyze the influence of soil water balance on flood spatial arrangements.

Materials and Methods

1. Study area

The study area is located in DelAzul creek basin (center of Pampa Ecoregion, Buenos Aires province, Argentina). This basin has an area of 6,237 km² and is crossed by permanent runoff path, highlighting Del Azul creek (which flows SW-NE) and its tributaries. Del Azul creekis drained by the artificial Channel 11; before its construction the creek discharged to the Salado River through a system of shallow lagoons and lowlands. The northern sector of the basin corresponds to a plain sub-environment, characterized by the extreme horizontality of its landscape. At local scale, there are numerous deflation basins with associated dunes currently occupied by wetlands, and longitudinal and parabolic dunes that are not very noticeable in the field (relative heights less than 0.7 m), as well as extensive areas of spillage similar to alluvial fans (Zarate & Tripaldi, 2012) observable in satellite images towards the NW of Del Azul creek. There, the drainage network is not integrated, it is scarcely dense, and its orientation tends to be subparallel with respect to Del Azul creek. General direction of surface and groundwater runoff is towards N-NE, presenting a groundwater flow with a general flat tendency and water gradients of approximately 1 m/km (Sala, González & Kruse, 1987).

Specifically, flooding patterns were analyzed in a geomorphologically homogeneous zone of the lower basin, which has an area of 854 km^2, with slopes ranging between 0.1-0.2%, without notable variations of the relief (Figure N°1). Sodic soils with poor drainage (Natracuols) dominate the area; more than 90% of the zone is used for livestock (average stocking rateper hectare = 1.1), and just over 2% for agriculture (INTA, 1992; Lanceta, Entraigas, de Dominicis & Vercelli, 2016). The study was developed along the year 2014. Daily rainfall and radiation data were taken from the weather station of National Meteorological Service (SMN) located 30 km far from the central point of the study area. Daily water table levels were

measured in the borehole N°12 (10 m depth) of the Large Plains Hydrology Institute monitoring network, which is located in the NE of the study area.

2. Daily water balance estimation

Water inputs less water outflows to the basin in a certain day is equal to the daily water excess or deficit of a basin (EXC or DEF). EXC or DEF, useful reserve (UR) and water table level for the selected dates were calculated from a daily water balance. Balance considers daily rainfall (P) and derives a portion of them as surface runoff (SR) according to the Curve Number method. Difference between P and SR infiltrates in the ground, and becomes part of moisture stored in soils. As long as soil moisture does not exceed its field capacity, real evapotranspiration (RET) grows from zero for null storage (equal to permanent wilting point) to RET = PET (potential evapotranspiration) for complete storage (field capacity). UR variation of day *i* is calculated as infiltrated water (rain or maximum infiltration capacity) minus PET of day *i* ($\Delta UR_i = P_i - PET_i$). Daily EXC or DEF is obtained as the sum of UR of day *i-1* plus UR variation of day *i* minus UR of day *i* ($EXC\ or\ DEF_i = UR_{i-1} + \Delta UR_i - UR_i$). If the field capacity is exceeded, soil cannot retain more water and this percolates to the aquifer. As the study area is a zone of plains with shallow groundwater levels, percolation becomes recharge without delay, making the water table rise, according to the specific yield of sediments (Nwankwor, Cherry & Gillham, 1984).

PET was calculated using the Penman-Monteith method recommended by the FAO, whose validity has been demonstrated for both wet and dry climates (Allen, Pereira, Raes & Smith, 1998). Balance parameters were adjusted according to soils features, vegetation and antecedent moisture in the study area (Field capacity = 27 %; Initial moisture = 35 %; Permanent wilting point = 12 %; Root exploration depth = 410 mm; UR = 61.50 mm; Initial reserve = 94.30 mm; CN = 72; Specific yield = 0.1).

3. Satellite images processing

Characterization of flooded areas using optical images is based on differences in the spectral response of soil and water, mainly in infrared wavelengths.While water absorbs a large part of the energy in near (NIR) and middle infrared (MIR), vegetation, soil and waterproof surfaces present a higher reflectance in those portions of the electromagnetic spectrum (Jensen, 2007; Xie, Luo, Xu, Pan & Tong, 2016). Various

methods have been developed for the extraction of flooded areas using optical satellite images (Huang, Chen, Zhang & Wu, 2018). Among the most widespread are the Normalized Difference Water Index (NDWI - Gao, 1996) and the modified NDWI, proposed by Xu (2006), which compute the normalized differences between reflectance in NIR and MIR, and green and MIR, respectively.

Despite the good performance of these indices in the characterization of water bodies and flooded areas (Liu, Yao & Wang, 2016; Xie et al., 2016), they have presented limitations when attempting to further characterize flooded areas of shallow, turbid or vegetated waters (Bustamante, Díaz-Delgado & Aragonés, 2005) as it occurs during water excess events in the study area. Consequently, band 6 (SWIR-1; 1.566-1.651 μm) of the Landsat 8 OLI sensor was chosen because it is less sensitive to water sediment load and is able to reflect subtle differences in it, which provides a greater ability to delineate water-soil boundary (Bustamante et al., 2005; Huang et al., 2018).

Flooding patterns were analyzed in 5 images of the LandSat 8 satellite (225-86), selected according to their availability and absence of clouds. Scenes used correspond to January 17th, March 22nd, June 10th, August 13th and November 17th. To delimit flooded patches in different images, we segment the histogram of band 6 according to intervals where both permanent and semi-permanent water bodies are identified, as well as waterlogged sites with shallow water. High-resolution satellite images available in Google Earth were used as support. Taking into account that the area is characterized by shallow water bodies that contain mixed water and vegetation pixels, we used values of surface reflectance that ranged between 0 and 0.15. Those pixels that were contemplated within these values were considered as class "water", while pixels with higher reflectance values were considered as class "no water". Through this procedure, five binary maps were obtained, for each selected date, with only two informational classes.

4. Landscape metrics calculation

In this study, we only analyzed the structure of class "water", that is, the sizes, shapes, quantities and spatial relationships between the patches that make it up, while patches of class "not water" constitute landscape matrix. Spatial configuration of patches of class “water” was analyzed in 15 square windows (20.25 km^2 each), repeating their location in each chosen date (see Figure N° 1).

In each window for each date, the following landscape metrics were calculated on class "water", using FragStat 4.1 (McGarigal, Cushman & Ene, 2012) (Details for metrics calculation in Supplementary material):

- Area metrics: they describe the size of patches and the number of edges. We selected the metrics Percentage of Landscape (PLAND) and Area (AREA).
- Aggregation metrics: they characterize the tendency of patches to be spatially aggregated, that is, to occur in large, aggregated, or "contagious" distributions.This property usually refers to landscape texture, describing the dispersion, subdivision and / or isolation of patches. We calculated metrics named Number of Patches (NP), Euclidean Nearest Neighbor Distance (EEN) and Connectance Index (CONNECT).
- Shape metrics: they distinguish between patches and landscapes based on global complexity, emphasizing objects geometry, but without discriminating particular morphologies. We chose the metrics Related Circumscribing Circle (CIRCLE) and Perimeter-area Ratio (PARA).

There are two basic types of metrics at class level: 1. Indexes that consider quantity and spatial configuration of the class, and 2. Distribution statistics that provide first and second order summaries of patch level metrics for each class.For the second case, class-level metrics are computed by synthesizing the aggregate distribution of patches of the same type, that is, summarizing the patch-level metrics for all the patches that make up the class. Metrics as PLAND, NP and CONNECT, describe the class, while AREA, PARA, CIRCLE and ENN, are computed at patch level. The latter, then, were synthesized for class "water" using the area-weighted average (AM). AM is equal to the sum of the metric value in the patch *ij* multiplied by the proportional abundance of the patch *ij* for all the patches of class *i*, that is:

$$AM = \sum_{j=1}^{n}\left[x_{ij}\left(\frac{a_{ij}}{\sum_{j=1}^{n} a_{ij}}\right)\right]$$

5. Data analysis

First, the dispersion of the values taken by each landscape metric we analyzed, and secondly, R^2Spearman coefficient (Myers & Well, 2003) between them was calculated. Then, a Principal Components Analysis (PCA) with Varimax rotation was carried out on the correlation matrix among the 7 metrics, considering values for the 75 cases (windows). Using PCA, the dimensionality of the data was reduced, the axes of

highest variation were found and the dispersion of the selected sites in principal components (PCs) was analyzed.

The spatial configuration of the flooded sites within each date was analyzed. For this, the average values of the windows on the PCswere compared between those located to the NW and those located to the SE of Del Azul creek. This comparison was made based on the Kolmogorov-Smirnov test.

Finally, we calculated Spearman's correlation coefficient between the medians ofthe windows for each date in the PCs, and the data obtained from the daily water balance (sum of EXC or DEF in the previous 30 days, UR, watertable level), to analyze the relationship between flooding patterns and the hydrological scenarios. All statistical analyzes were performed using R (R Core Team, 2018).

Results

1. Daily soil water balance

During 2014 accumulated rainfall totaled 1129 mm, higher than the historical average for the period recorded in the weather station SMN (915 mm – period 1901-2018). When monthly distribution of rainfall is analyzed, its noticeable the increase of accumulated rainfall in autumn (March, April and May) and winter (June, July and August) for the analyzed period compared with historical data, while there are no considerable differences during spring (September, October and November) and summer (December, January and February) (Figure N° 2).

As it usually happens in the region, during the spring end and summer the system went through periods of water deficit where water outflows by RET exceeded the inputs to the system. On the other hand, in autumn and winter the situation is totally opposite: P exceeded losses due to evaporation and RET, which raised watertable levels and increased moisture content of soils. If rainfall is particularly abundant at this time of year, then water accumulates over the surface (Figure N°3).

The images of January 17th (Figure N° 4.A.) and November 17th correspond to deficit periods, while those taken on June 10th and August 13th (Figure N° 4.C.) belong to water excess situations. The image of March

22nd represents an intermediate scenario (Figure N° 4.B.): it temporarily coincides with end of summer and beginning of autumn, when losses due to evaporation and RET begin to decrease, and P and UR in soils usually increase.

2. Flooding patterns in contrasting hydrological situations

The PCA concluded in two components with eigenvalues higher than 1, which represent 76.98% of total variance. R^2 Spearman coefficients between the original variables were all less than 0.6, with the exception of the PLAND-CIRCLE pair (0.61, $p < 0.05$). PC1 presented positive correlation with PLAND, AREA and CIRCLE, and negative with PARA (Table N° 1), reflecting the variation in area and shape of the patches included in class "water". In this way, as values in PC1 increase, windows present a higher percentage of the landscape occupied by water, more elongated and linear patches, with larger average areas and lower perimeter-surface relationship.

On the other hand, PC2 correlated positively with ENN and CONNECT, and negatively with NP, showing the dispersion taken by aggregation metrics: the higher the values in PC2, windows show lower number of patches, greater average Euclidean distances to nearest neighbor and greater number of connections between patches than maximum possible for each one. Thus, PC1 reflected variability in percentage of flooded landscape, area and shape of the patches, and PC2 reflected dispersion in aggregation metrics.

Windows' PCs scores (Figure N ° 5) showed that in PC1, August windows and some of June windows took positive values, because they present a higher percentage of the landscape occupied by water, more elongated patches, with a higher average area and a lower perimeter / surface ratio. January, March and November windows showed negative values on this component. At the same time, in PC2 all January windows took positive values for having fewer patches, longer Euclidean distances to the nearest neighbor, and greater number of connections between patches. On the other hand, all June windows showed negative values; while for March, August and November both positive and negative values were observed.

Heterogeneity in flooding patterns within the same date was analyzed by comparing means for each group of windows (8 located to the NW vs 7 located to the SE of Del Azul creek) in PC 1 and 2 (Table N° 2 and 3, respectively).

Taking into account that PC1 synthesized area and shape metrics, and that PC2 reflected dispersion in aggregation indexes, results showed that as the system became saturated the two zones have different behaviors in the metrics considered. In deficit situations, there were no differences between zones, since the lack of water in the system operates at the basin scale, independently of the particularities of each part of the lower basin. In intermediate situations, as in March 2014, differences were reflected in PC2: the NW zone presented higher number of patches with smaller distances between them, but do not differ from SE zone in the percentage of flooded landscape or the average area of patches. Finally, in excess water situations, there were significant differences between average values of NW and SE zones in PC1, evidenced in the higher percentage of flooded landscape and higher area of patches at NW. However, medians in PC2 only recorded significant differences in August, but not in June: this shows that the NW zone is saturated at times of greater water excess (like August), which generates the patches fusion, causing the registration of fewer patches and higher distances between them.

3. Soil water balance influence on flooding patterns

Spearman's correlation coefficients between soil water balance and windows scores in PCs gave the following results: 1. Positive correlation between medians for each date on PC1 and simulated water table levels (0.90; $p < 0.05$) (Figure N° 6.A.). 2. Negative correlation between medians for each date on PC2 and the sum of EXC or DEF in previous 30 days prior to image date (0.90; $p < 0.05$) (Figure N° 6.B). 3. Negative correlation between medians for each date on PC2 and UR in soils (0.87; $p < 0.1$) (Figure N ° 6.B.).

In this way, area and shape of patches with surface water were positively related to fluctuations of watertable level, presenting larger and longer patches as the aquifer recharges. On the other hand, patches

aggregation was negatively associated with the accumulated EXC or DEF, and with the UR in soil. Thus, the greater the accumulated excesses and the UR, the more patches with smaller distances between them.

Discussion

Accumulated rainfall during 2014 caused a water excess in the system concentrated in autumn and winter, which generated water accumulation over land surface and water table levels rise (fluctuation of 1.97 y 1.95 m in observed and simulated water table levels, respectively). While groundwater is often perceived as a relatively static reservoir (Alley, Healy, LaBaugh & Reilly, 2002, Sophocleous, 2002), its shallower component makes an important contribution to the variation of total water storage in flat landscapes with water tables levels near surface. In addition, as pointed out by Aragón et al. (2010), this reservoir shows fast storage changes: in the analyzed area, net recharge was 185 mm between the beginning of autumn (March 15th) and the end of winter (August 31st). Surface water storage also recorded rapid fluctuations: less than 1% of the area was flooded in mid-summer (image January 17th), 24.6% at the end of winter (image August 13th) and 4.7% at the end of spring (image November 17th). The response speed of groundwater and surface water reservoirs, whose changes are perceptible in weeks or months, allows us to consider the hydrological situation of the period autumn-winter 2014 as a fast flood, according to the classification for the Pampa region proposed by Kuppel, Houspanossian, Nosetto and Jobbágy (2015).

Unlike happens in other plain landscapes, such large rivers floodplains of South America (Hamilton, 2002), here water excesses are not seasonal, but depend on the interannual climatic variability observed in the region, controlled mainly by the ENSO phenomenon (Garreeaud et al., 2009). At the SMN weather station used for soil water balance estimation, for the period 1901-2018, records indicate that there were 21 years with rainfall greater than 1100 mm (including 2014) and 14 with rainfall less than 700 mm, which shows that climate variability is not something exceptional.

Regarding to flooding patterns in contrasting hydrological situations, PCA indicated that the median values taken by the windows of each date in PCs 1 and 2 had a similar behavior, with possible threshold-driven performance. Within PC 1, August windows standout due to their high values and to a lesser extent those of June; the other dates presented similar (low) medians values. In agreement with this, August was the moment with most water excess and shallow watertable levels, and June the one that follows. However,

there were no differences in area or shape of the patches with surface water when comparing deficit or intermediate periods, despite the variation deficits magnitude.

Windows medians for each date on PC 2 showed that for January, March, June and November values on the axis decreased as accumulated deficit/excesses and UR in soils increased, that is, number of patches increased and distances between them decreased. Unlike in August, when the system was with water excess, shallow watertable levels and high UR in soils, number of patches decreased and average distance between them increased. In this way, surface water coverage increased by the development of new patches; as excess water accumulated, patches became larger and finally collapsed and merged, as reported by other studies (Aradas, Lloyd, Wicks & Palmer, 2002; Aragón et al., 2010). Thus, although lateral movements of water are assumed to be negligible in areas with very low topographic gradient (Ferone & Devito, 2004; Winter, 1999) as suggested by available flow data for the Salado River reported by Kuppel et al. (2015), their importance changed during flood events when a structural connectivity threshold is crossed. Hence, surface runoff on a local scale can be an important driver of water bodies coalescence.

Internal heterogeneity observed in the study area in water excess situations coincides with the hypothesis of the existence of old alluvial fans in the northern Tandilia piedmont (Zarate & Tripaldi, 2012), which are evident to the NW of Del Azul creek in satellite images. Currently, they would be controlling the expression of the drainage network in the area, which is why in excess situations they act as preferential runoff ways, being responsible for the possible threshold behavior and the patch fusion observed in August. These fans are not recognizable in the field: soils profiles observed in the area do not show alluvial deposits or evidence of water erosion (Vercelli, 2018). Therefore, it is considered that these fans could have formed during the Pleistocene, prior to the deposit of Postpampeano sediments (Later Pleistocene – Holocene). The situation to the SE of the creek is different, since alluvial fans are not recognized either in images or in the field. A possible explanation is that aeolian reactivation occurred during the Late Middle Holocene would be partially responsible for depositing greater thickness of sediments to the SE of Del Azul creek, softening the expression of old drainage paths. Then, ancient landforms barely noticeable in the field control the expression of drainage network, as it occurs in other areas of the Argentine Pampas (Viglizzo & Frank, 2006). The hydrologic landscape concept proposed by Winter (2001), where fundamental units are defined considering its land surface form, geologic framework, and climatic setting, showing general movement of surface water, groundwater, and atmospheric water, respectively, is difficult

to apply in extremely flat landscapes like the one analyzed here if the used tools are not adequate to highlight these characteristics, especially if the climatic conditions are relatively homogeneous for the selected area, and there is evident interaction between groundwater and surface water.

From the results presented here is clear that fluctuations in water table levels and the sum of accumulated EXC or DEF in previous 30 days seem to be the parameters that best related with flood spatial configuration, for their good correlation with PCs 1 and 2, respectively. On the other hand, relationship between UR and flood spatial configuration is less strong than the other two variables considered, because its particular behavior: although there is water excess accumulated in the system, it can take low values; and whatever the deficit magnitude its value cannot be less than zero.

Linkages between flooding patterns and hydrological variables in plains areas have been little explored in the region: studies carried out by Hamilton (2002) and Hamilton et al. (2004) in large floodplains relate flooded area with river stage, while Kuppel et al. (2015) analyzed the correlation between terrestrial water storage and surface water cover during two significant flood events in Pampa region. In the study presented here, flooding patterns are characterized by landscape metrics, in order to extract more information than simply the percentage of flooded area. Unlike the result reported by Kuppel et al. (2015) and Hamilton (2002), which found low linear correlation between the proportion of flooded area and the terrestrial water storage and river stage, respectively, and suggested a delay as explanation, our results showed good correlation between water table levels and the area and shape of patches with surface water (PC 1). Despite the low permeability of soils and sediments in the region (Taboada, Damiano & Lavado, 2009), the above suggests a good connection between groundwater and surface in the studied area. Differences can be attributed, mainly, to scale used for the analysis, and methods for water storage estimation. Data uncertainty results from sampling, measurement and interpretation errors in the observed data (Renard, Kavetski, Kuczera, Thyer & Franks, 2010).

There is a large amount of recent work using landscape metrics for analyzing hydrological patterns and processes, many of them with the aim of studying flow connectivity (Epting et al., 2017; Gao et al., 2018; Larsen, Ma & Kaplan, 2017; Van Nieuwenhuyse et al., 2015; Yuan et al., 2015; among others). In these studies, metrics that explicitly consider topography are applied, and main conclusions indicated that flow-explicit metrics are the most appropriate to analyze connectivity, being that other pattern metrics based solely on geometry are poor predictors of connectivity and hydroperiod.

However, the results obtained here after applying spatial configuration metrics based on patches geometry indicate that these metrics are useful for describing structural connectivity in flat areas, where classical indexes that consider topography are not easily applicable due to the extremely soft relief. As Van Nieuwenhuyse et al. (2015) said that metrics that took into account both distance and aggregation performed best, here it is evident that the joint consideration of area, shape and aggregation metrics is a useful, fast and low cost tool to characterize the flood spatial arrangements in contrasting hydrological situations, in areas with very subtle topographic gradients.

Summary and conclusions

As proposed by Blöschl and Grayson (2000), spatial patterns in hydrological processes are a rich source of variability, which in some cases are obvious to the observer, but not in others. Manifested heterogeneity comes from the spatial arrangement of the hydrologically relevant variables. Understanding such spatial arrangement is extremely important for designing appropriate sampling strategies, for interpreting data correctly, for constructing and / or applying dynamic models, and finally for using this data in the prediction of basin behavior.

Results of this work show that the applied tools are useful to highlight spatial patterns of surface water accumulation, especially in areas of low relief or in those cases where data is scarce or insufficient. Its advantage in terms of low cost is remarkable, which is a great benefit in exploratory analyzes carried out prior to the instrumentation of areas of interest. In relation to the above, it is notable the high correlation observed between soil water balance and the spatial configuration of flooded sites on different scenarios. This is another reason to apply GIS-derived metrics to analyze, explain and predict spatial variability in catchments, as other authors proposed (Van Nieuwenhuyse et al., 2011; Epting et al., 2017), especially when data and instruments are scarce.

Although various hydrological models are developed based on topographic information, the fractal patterns of geomorphology may inform modelers more about how water interacts with landscapes (Rodríguez-Iturbe & Rinaldo, 2001), causing the nonlinearity of rainfall-runoff processes. Spatial observations have great importance to improve understanding of hydrological responses in basins, but the measured (or interpolated) patterns have limited utility without a conceptual framework within which they can be explained (Grayson & Blöschl 2000). From this work, the expression of two zones with different

hydrological behavior arises within Del Azul creek lower basin, which can be explained from the hypothesis of ancient alluvial fans in the northern Tandilia piedmont controlling drainage networks.

Acknowledgements

We thank Mariana Oyarzabal for the review comments on the manuscript, and Luisa Fajardo Gonzalez for helping to improve figure's quality. We also thank the anonymous referees, whose valuable review helped improve and clarify this manuscript.

References

Allen R. G., Pereira L. S., Raes D., & Smith M. 1998. Crop evapotranspiration - Guidelines for computing crop water requirements. *FAO Irrigation and drainage paper56.* FAO - Food and Agriculture Organization of the United Nations, Rome.

Alley M.W., Healy R.W., LaBaugh J.W., & Reilly, T.E. 2002. Flow and storage in groundwater systems. *Science, 296*, 1985–1990. http://doi:10.1126/science.1067123

Aradas R., Lloyd J., Wicks J., & Palmer J. 2002. Groundwater problems in low elevation regional plains: The Buenos Aires Province example. In: *Groundwater and Human Development*, Bocanegra E., Martinez D., & Massone H (eds). Taylor & Francis. London. 613–623.

Aragón R., Jobbágy G., & Viglizzo E. 2010. Surface and groundwater dynamics in the sedimentary plains of the Western Pampas (Argentina). *Ecohydrology, 4 (3),* 433–447. http://doi:10.1002/eco.149.

Biancamaria S., Bates P., Boone A., & Mognard N. 2009. Large-scale coupled hydrologic and hydraulic modelling of the Ob river in Siberia. *Journal of Hydrology, 379 (1–2),* 136–150. http://doi:10.1016/j.jhydrol.2009.09.054.

Blöschl G. & Grayson R. Chapter 2. Spatial Observations and Interpolation. In: *Spatial patterns in catchment hydrology: observations and modeling*, Grayson R. & Blöschl G. (eds). Cambridge University Press, UK. 17-50.

Bracken L. J. & Croke J. 2007. The concept of hydrological connectivity and its contribution to understanding runoff dominated geomorphic system. *Hydrological Processes, 21,* 1749-1763. https://doi.org/10.1002/hyp.6313.

Bustamante J., Díaz-Delgado R., & Aragonés D. 2005. Determinación de las características de masas de agua someras en las marismas de Doñana mediante teledetección. *Revista de Teledetección, 24*, 107-111.

Dingman S.L. 2015. *Physical hydrology*. Waveland press, Illinois.

Epting S., Hosen J., Alexander C., Lang M., Armstrong A., & Palmer M. 2017. Landscape metrics as predictors of hydrologic connectivity between Coastal Plain forested wetlands and streams. *Hydrological Processes, 32*, 516–532. http://DOI:10.1002/hyp.11433

Fajardo González L.F. 2017. Planteamiento y aplicación de técnicas de corrección del modelo digital de elevación SRTM en la zona serrana de la cuenca del arroyo del Azul. MgSc Thesis. Universidad Nacional del Centro de la Provincia de Buenos Aires, Buenos Aires, Argentina.

Fan Y., Li H., & Miguez-Macho G. 2013. Global patterns of groundwater table depth. *Science, 339 (6122),* 940–943. http://doi:10.1126/science.1229881.

Ferone J. & Devito K. 2004. Shallow groundwater-surface water interactions in pond-peatland complexes along a Boreal Plains topographic gradient. *Journal of Hydrology, 292*,75–95. http://DOI:10.1016/j.jhydrol.2003.12.032

Fuschini Mejía M.C. 1994. *El agua en las llanuras*. International Hydrological Program. UNESCO, Montevideo, Uruguay.

Gao B. 1996. NDWI – A normalized difference water index for remote sensing of vegetation liquid water from space. *Remote Sensing of Environment, 58 (3),* 256-266. https://doi.org/10.1016/S0034-4257(96)00067-3.

Gao H., Sabo J., Chen X., Liu Z., Yang Z., Ren Z., & Lui M. 2018. Landscape heterogeneity and hydrological processes: a review of landscape-based hydrological models. *Landscape Ecology, 33*, 1461–1480. https://doi.org/10.1007/s10980-018-0690-4

Garreaud R.D., Vuille M., Compagnucci R. &, Marengo J. 2009. Present-day South American climate. *Palaeogeography, Palaeoclimatology, Palaeoecology, 281,* 180-195. https://doi.org/10.1016/j.palaeo.2007.10.032.

Grayson R. & Blöschl G. 2000. Chapter 3. Spatial Modelling of Catchment Dynamics. In: *Spatial patterns in catchment hydrology: observations and modeling,* Grayson R. & Blöschl G. (eds). Cambridge University Press, UK. 51-81.

Hamilton S. 2002. Comparison of inundation patterns among major South American floodplains. *Journal of Geophysics Research, 107 (D20), 8308, LBA5*, 1–14. http://doi:10.1029/2000JD000306.

Hamilton S., Sippel S., & Melack J. 2004. Seasonal inundation patterns in two large savanna floodplains of South America: The Llanos de Moxos (Bolivia) and the Llanos del Orinoco (Venezuela and Colombia). *Hydrological Processes, 18 (11),* 2103–2116. http://doi:10.1002/hyp.5559.

Huang C., Chen Y., Zhang S., & Wu J. 2018. Detecting, extracting, and monitoring surface water from space using optical sensors: a review. *Reviews of Geophysics, 56,* 333-360. https://doi.org/10.1029/2018RG000598.

INDEC, 2008. Censo Nacional Agropecuario 2008. Report CNA 2008, Instituto Nacional de Estadística y Censos, Buenos Aires, Argentina.

INDEC, 2010. Censo Nacional de Población, Hogares y Viviendas 2010. Instituto Nacional de Estadística y Censos, Buenos Aires, Argentina.

INTA. 1992. Carta de Suelos de la República Argentina, Buenos Aires, Argentina: Hojas 3760-10 (Cacharí), y 3760-16 (Azul), 1:50,000. Instituto Nacional de Tecnología Agropecuaria, Buenos Aires.

Jensen J. R. 2007. *Remote Sensing of the Environment: An Earth Resource Perspective*. Prentice Hall, Upper Saddle River, N.J.

Jobbágy E., Nosetto M., Santoni C., & Baldi G. 2008. El desafío ecohidrológico de las transiciones entre sistemas leñosos y herbáceos en la llanura Chaco-Pampeana. *Ecología Austral, 18 (3),* 305–322.

Jones K., Poole G., O' Daniel S., Mertes L. &, Stanford J. 2007. Surface hydrology of low-relief landscapes: Assessing surface water flow impedance using LIDAR-derived digital elevation models. *Remote Sensing of Environment, 112,* 4148-4158. https://doi.org/10.1016/j.rse.2008.01.024.

Kuppel S., Houspanossian J., Nosetto M., & Jobbágy E. 2015. What does it take to flood the Pampas?: Lessons from a decade of strong hydrological fluctuations. *Water Resources Research, 51,* 2937–2950. http://doi:10.1002/2015WR016966.

Lanceta M., Entraigas I., de Dominicis H., & Vercelli N. 2016. Determinación de la superficie potencial ganadera a través del uso de sistemas de información geográfica. *Geofocus: Asociación de Geógrafos Españoles, 18,* 47-63. http://dx.doi.org/10.21138/GF.464

Larsen L., Ma J., & Kaplan D. 2017. How important is connectivity for Surface water fluxes? A generalized expression for flow through heterogeneous landscapes. *Geophysical Research Letters, 44 (10),* 349–358. https://doi.org/10.1002/2017GL075432

Liu Z.,Yao Z., & Wang R. 2016. Assessing methods of identifying open water bodies using Landsat 8 OLI imagery. *Environmental Earth Sciences,75(10),*1-13. https://doi.org/10.1007/s12665-016-5686-2

Magrin G.O., Travasso M.I., & Rodríguez, G.R. 2005. Changes in climate and crop production during the 20th century in Argentina. *Climatic Change*, *72*, 229–249. https://doi.org/10.1007/s10584-005-5374-9.

Matteucci S.D. 2012. Ecorregión Pampa. In: *Ecorregiones y Complejos Ecosistémicos Argentinos*, Morello J., Matteucci S.D., Rodríguez A.F., & Silva, M. (Eds.) Orientación Gráfica Editora, Buenos Aires. 391-445.

McGarigal K., Cushman S.A. & Ene E. 2012. FRAGSTATS v4: Spatial Pattern Analysis Program for Categorical and Continuous Maps. *Computer software*. University of Massachusetts, Amherst. Available at: http://www.umass.edu/landeco/research/fragstats/fragstats.html

Myers J.L. & Well A.D. 2003. *Research Design and Statistical Analysis* (2nd ed.). Lawrence Erlbaum, NJ, USA.

Nwankwor G.I., Cherry J.A., & Gillham R.W. 1984. A Comparative Study of Specific Yield Determinations for a Shallow Sand Aquifer. *Groundwater*, 22 (6), 764-772. https://doi.org/10.1111/j.1745-6584.1984.tb01445.x

Pereyra F. 2003. *Ecorregiones de la Argentina*. Servicio Geológico Minero Argentino, Buenos Aires.

Pickett S.T. & Cadenasso M.L. 1995. Landscape ecology: spatial heterogeneity in ecological systems. *Science*, *239*, 331-334.

R Core Team. 2018. *R: A language and environment for statistical computing*. R Foundation for Statistical Computing. Vienna, Austria. https://www.r-project.org/

Renard B., Kavetski D., Kuczera G., Thyer M., & Franks, S. 2010. Understanding predictive uncertainty in hydrologic modeling: The challenge of identifying input and structural errors. Water Resources Research, 46, W05521, 1-22. http://doi:10.1029/2009WR008328

Rodríguez-Iturbe I. & Rinaldo A. 2001. Fractal river basins: chance and self-organization. Cambridge University Press, Cambridge.

Sala J.M., González N., & Kruse E. 1987. *Investigación hidrológica de la cuenca del arroyo Azul, provincia de Buenos Aires. Report 37*, Scientific Research Commission of Buenos Aires province, La Plata, Argentina.

Scarpati O.E. & Capriolo A.D. 2013. Sequías e inundaciones en la provincia de Buenos Aires (Argentina) y su distribución espacio-temporal. *Investigaciones Geográficas*, *82*, 38-51.

Schröder B. 2006. Pattern, process, and function in landscape ecology and catchment hydrology – how can quantitative landscape ecology support predictions in ungauged basins? *Hydrology and Earth System Sciences*, *10*, 967–979.

Scioli C. 2009. Modelación del escurrimiento superficial en áreas de llanura: Implementación y calibración de un modelo distribuido de grilla. MgSc Thesis – Universidad Nacional de Rosario, Rosario, Argentina.

Scioli C. & Villanueva A. 2011. Modelación hidrológica de grilla en zonas de llanura: movimiento multidireccional del agua. *Aqua-Lac*, *3 (1)*, 1-8.

Sivapalan M. 2005. Pattern, Process and Function: Elements of a Unified Theory of Hydrology at the Catchment Scale. In: *Encyclopedia of Hydrological Sciences, vol. 1, part 1*, Anderson M.G. (ed). John Wiley, Hoboken, N. J. 193–219.

Sophocleous M. 2002. Interactions between groundwater and surface water: the state of the science. *Hydrogeology Journal*, *10*, 52–67. https://doi.org/10.1007/s10040-001-0170-8

Taboada M., Damiano F., & Lavado R. 2009. Inundaciones en la Región Pampeana. Consecuencias sobre los suelos. In: *Alteraciones de la fertilidad de los suelos: el halomorfismo, la acidez, el hidromorfismo y las inundaciones*, Taboada M. & Lavado R. (eds.). Editorial Universidad de Buenos Aires. 103–127.

Tetzlaff D., Soulsby C., Bacon P.J., Youngson A.F., Gibbins C., & Malcolm I.A. 2007. Connectivity between landscapes and riverscapes — a unifying theme in integrating hydrology and ecology in catchment science? *Hydrological Processes*, *21*, 1385–1389. https://doi.org/10.1002/hyp.6701.

Turnbull L., Wainwright J., & Brazier R.E. 2008. A conceptual framework for understanding semi-arid land degradation: ecohydrological interactions across multiple-space and time scales. *Ecohydrology*, *1*, 23-34. https://doi.org/10.1002/eco.4.

Van Nieuwenhuyse B.H., Antoine M., Wyseure G., & Govers G. 2011. Pattern-process relationships in surface hydrology: hydrological connectivity expressed in landscape metrics. *Hydrological Processes, 25*, 3760–3773. https://doi.org/10.1002/hyp.8101.

Vercelli N. 2018. Heterogeneidad del paisaje en la cuenca inferior del arroyo del Azul, provincia de Buenos Aires. PhD Thesis. Universidad Nacional de Mar del Plata, Mar del Plata, Argentina.

Viglizzo E. & Frank F. 2006. Ecological interactions, feedbacks, thresholds and collapses in the Argentine Pampas in response to climate and farming during the last century. *Quaternary International, 158 (1),* 122–126. http://doi:10.1016/j.quaint.2006.05.022.

Western A.W., Bloschl G., & Grayson R.B. 2001.Toward capturing hydrologically significant connectivity in spatial patterns. *Water Resources Research, 37,* 83–97. https://doi.org/10.1029/2000WR900241.

Winter T.C. 1999. Relation of streams, lakes, and wetlands to groundwater flow systems. *Hydrogeology Journal, 7,*28–45. http://doi:10.1007/s100400050178.

Winter T.C. 2001. The concept of hydrologic landscape. *Journal of the American Water Resources Association, 38 (2),* 335-349.

Xie H., Luo X., Xu X., Pan H., & Tong X. 2016. Evaluation of Landsat 8 OLI imagery for unsupervised inland water extraction. *International Journal of Remote Sensing, 37(8),* 1826-1844.

Xu H. 2006. Modification of normalized difference water index (NDWI) to enhance open water features in remotely sensed imagery. *International Journal of Remote Sensing, 27(14),* 3023-3033.

Yuan J., Cohen M., Kaplan D., Acharya S., Larsen L., & Nungesser M. 2015. Linking metrics of landscape pattern to hydrological process in a lotic wetland. *Landscape Ecology, 30 (10),* 1893-1912.

Zárate M. & Tripaldi A. 2012. The Aeolian system of central Argentina. *Aeolian Research, 3,* 401-417. http://doi:10.1016/j.aeolia.2011.08.002.

Data Availability Statement

Data openly available in a public repository that does not issue DOIs

The data that support the findings of this study are openly available in Base de Datos Hidrológicos (BDH) at http://www.azul.bdh.org.ar, reference number BDH 3.0.0-RC2.

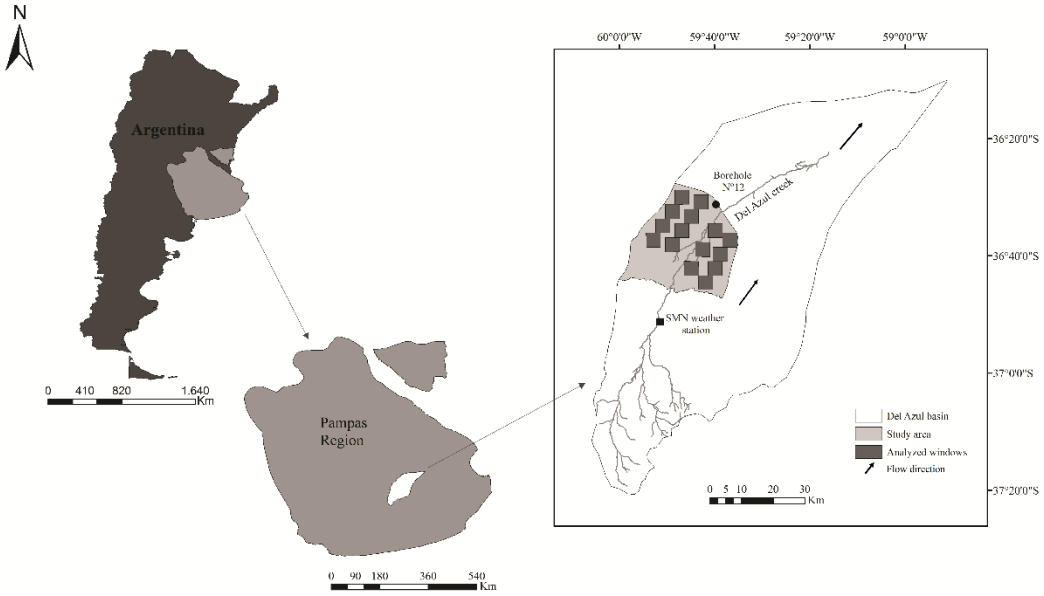

Figure 1. Study area. Location of the National Meteorological Service (SMN) weather station, borehole N° 12 and square windows used to calculate landscape metrics are shown.

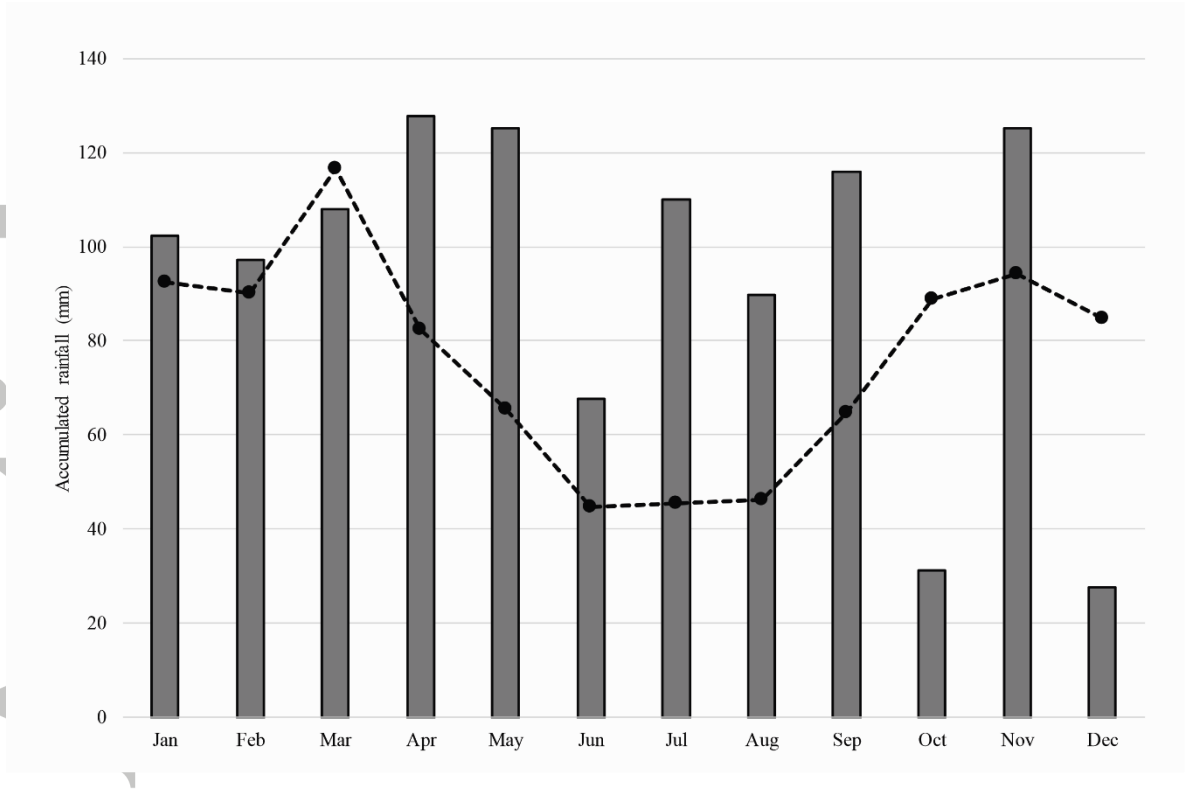

Figure 2: Monthly rainfall record in the SMN weather station. Rainfall during 2014 (grey bars) and historical averages (black dots) are shown.

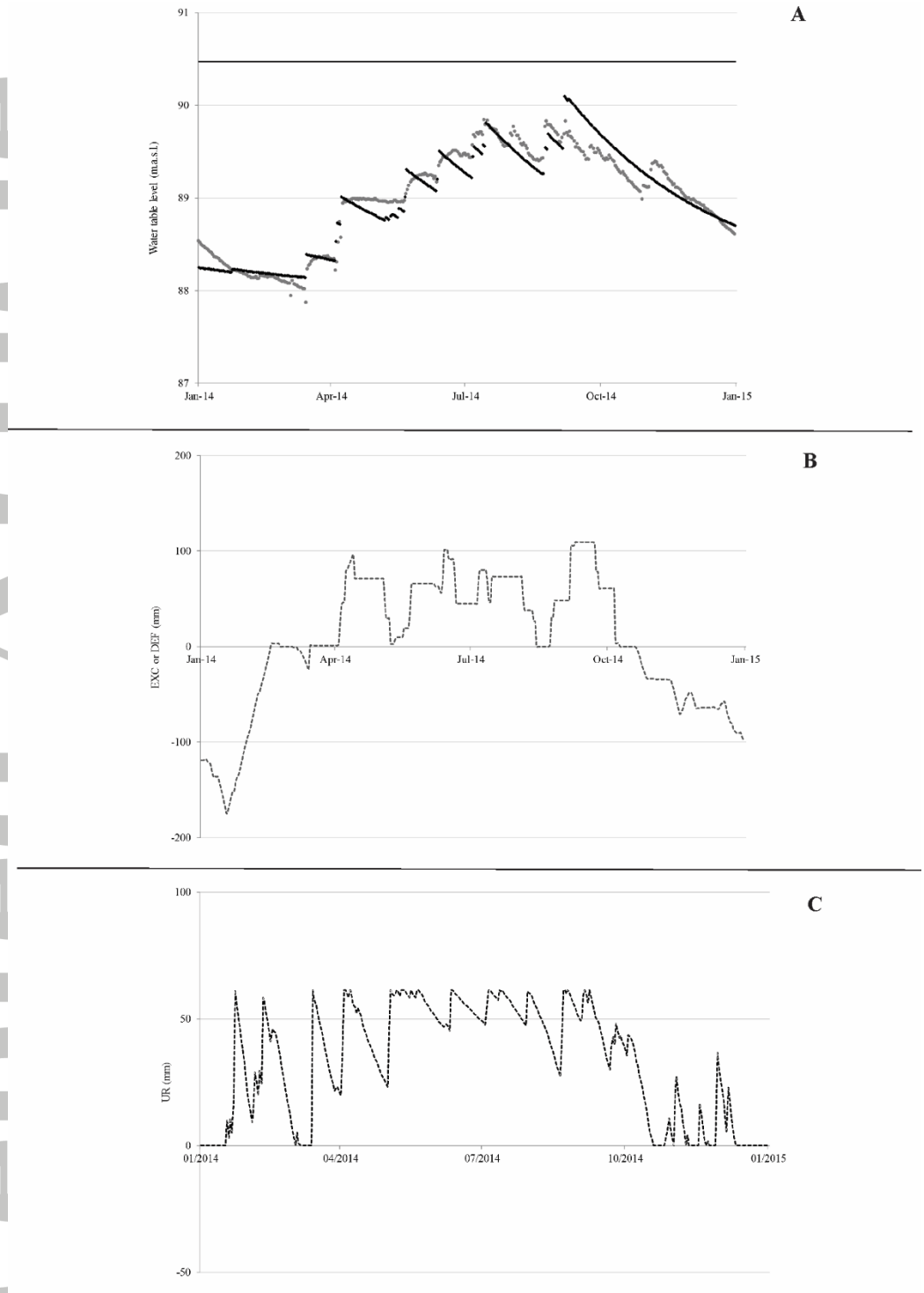

Figure 3. Water balance in 2014. A. Watertable level evolution. Simulated levels (grey dots). Observed levels (black dots). Land surface (continuous line). B. Sum of EXC or DEF in previous 30 days. C. Daily UR in soils.

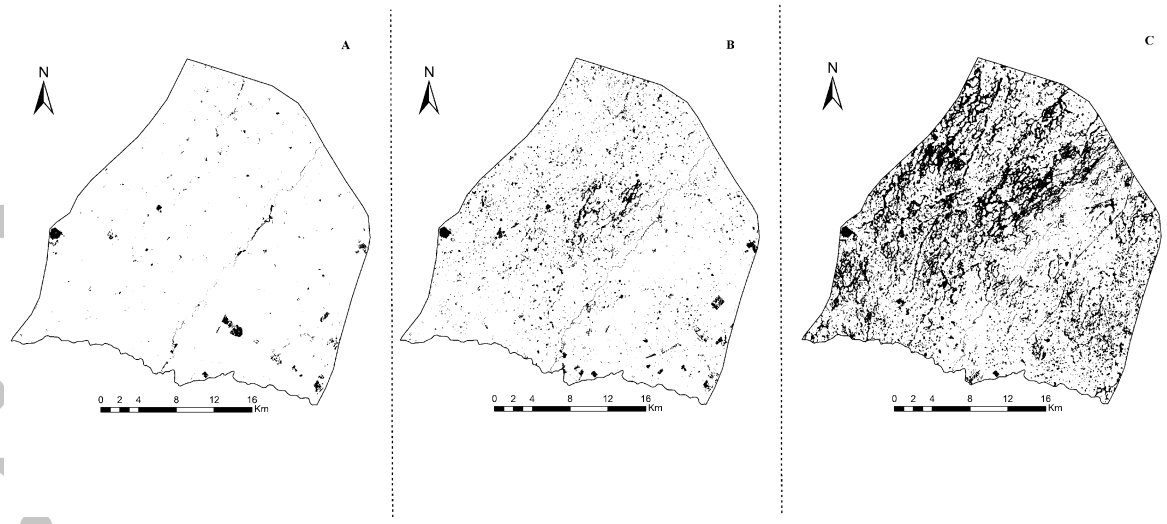

Figure 4: Binary maps obtained after classifying LandSAT images. Class “water” (black pixels). Class “no water” (white pixels) A. January 17th, 2014. B. March 22nd, 2014. C. August 13th, 2014.

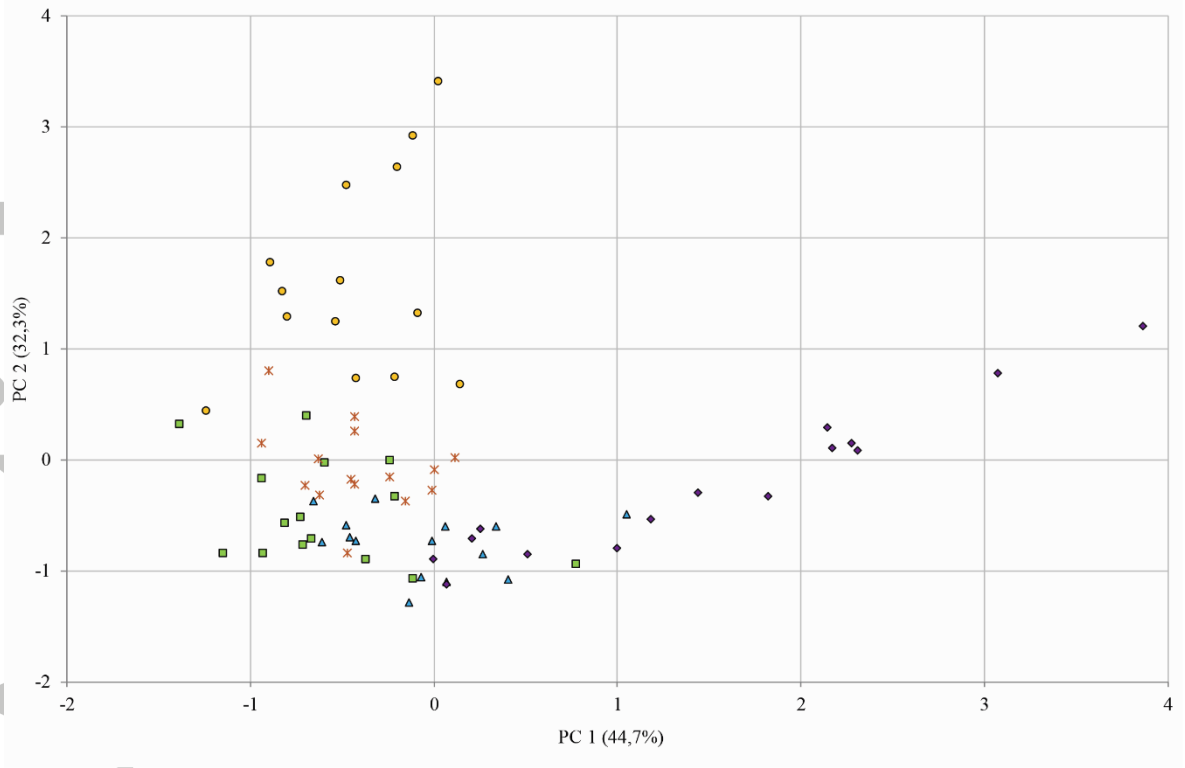

Figure 5. Windows' scores in PC 1 and 2. January (circles). March (squares). June (triangles). August (diamonds). November (crosses).

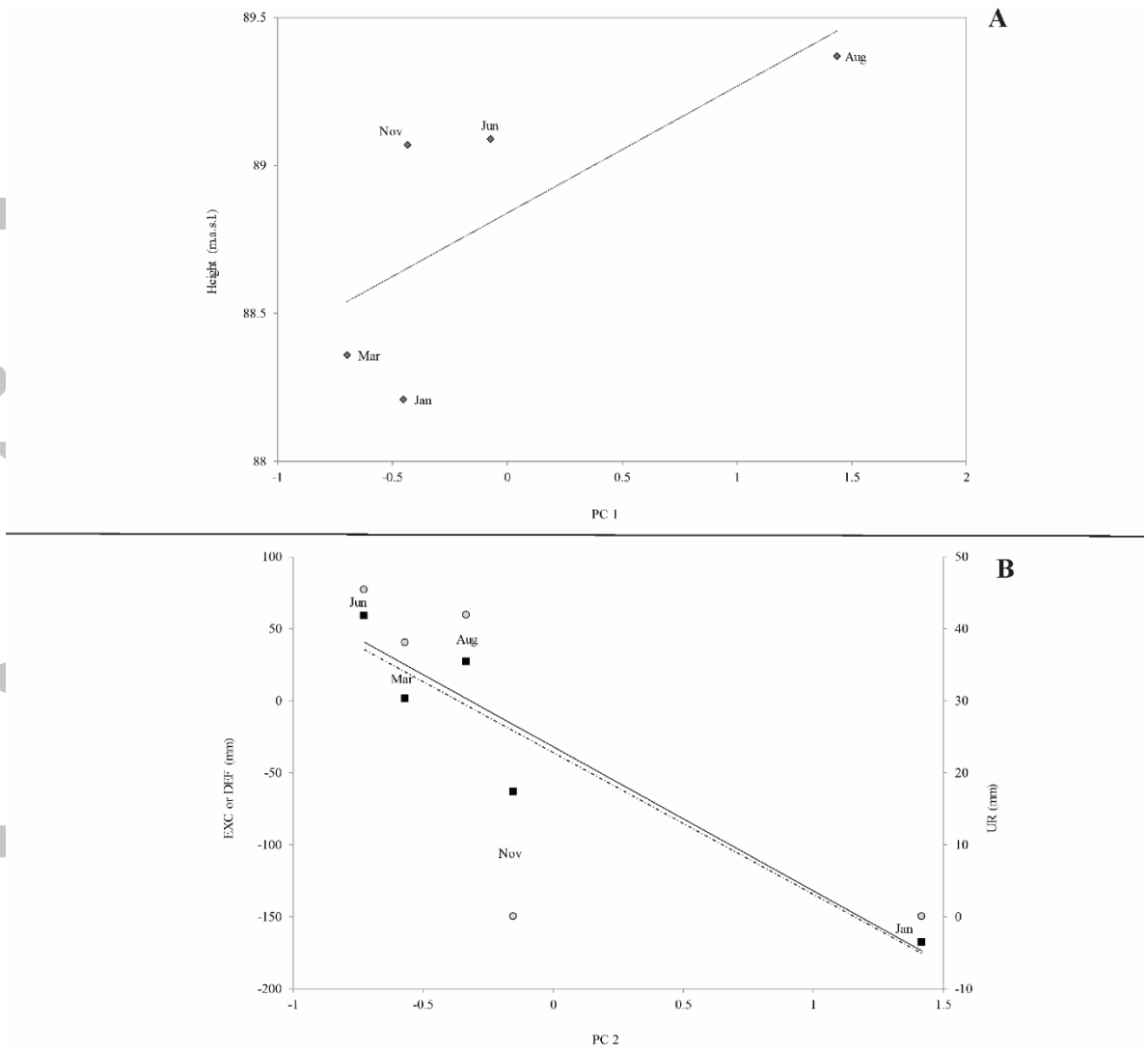

Figure 6: Relationship between water balance and windows medians per date on PC 1 and 2. A. Simulated watertable levels vs PC1 (diamond). B. Sum of deficit and excess for previous 30 days (black squares) and daily UR (gray circles) vs PC2.

Table N° 1: Factor Loadings for variables after Varimax rotation (Loadings> 0,7 indicated in bold).

	PC 1	PC 2
PLAND	**0,930**	-0,268
NP	0,242	**-0,866**
AREA	**0,849**	0,135
PARA	**-0,776**	0,342
CIRCLE	**0,835**	-0,189
ENN	-0,425	**0,708**
CONNECT	0,030	**0,873**
Expl.Var	3,129	2,259
Prp.Totl	0,447	0,322

Table N°2: Comparison between windows means of NW and SE zones in PC1 applying Kolmogorov-Smirnov test ($p < 0,01$ indicated in bold).

	NW Group		SE Group		Max. Difference	p-level
	Mean	Std.Dev.	Mean	Std.Dev.		
January	-0,521	0,432	-0,335	0,347	0,250	0,9587
March	-0,500	0,606	-0,687	0,407	0,250	0,9437
June	0,237	0,382	-0,410	0,240	0,857	**0,0028**
August	2,386	0,755	0,457	0,463	1,000	**0,0002**
November	-0,300	0,314	-0,561	0,174	0,625	0,0619

Table N°3: Comparison between windows means of NW and SE zones in PC2 applying Kolmogorov-Smirnov test ($p < 0,01$ indicated in bold).

	NW Group		SE Group		Max. Difference	p-level
	Mean	Std.Dev.	Mean	Std.Dev.		
January	1,854	1,056	1,332	0,651	0,458	0,3515
March	-0,830	0,151	-0,043	0,329	1,000	**0,0006**
June	-0,836	0,282	-0,654	0,257	0,357	0,6216
August	0,248	0,520	-0,791	0,196	1,000	**0,0002**
November	-0,141	0,164	0,009	0,534	0,429	0,38736